

# Local computation of angular velocity in rotational visual motion

José F. Barraza and Norberto M. Grzywacz

*Department of Biomedical Engineering and Neuroscience Graduate Program, University of Southern California, University Park, OHE 500, Los Angeles, California 90089-1451*

Received November 7, 2002; revised manuscript received March 27, 2003; accepted March 27, 2003

Retinal images evolve continuously over time owing to self-motions and to movements in the world. Such an evolving image, also known as optic flow, if arising from natural scenes can be locally decomposed in a Bayesian manner into several elementary components, including translation, expansion, and rotation. To take advantage of this decomposition, the brain has neurons tuned to these types of motions. However, these neurons typically have large receptive fields, often spanning tens of degrees of visual angle. Can neurons such as these compute elementary optic-flow components sufficiently locally to achieve a reasonable decomposition? We show that human discrimination of angular velocity is local. Local discrimination of angular velocity requires an accurate estimation of the center of rotation within the optic-flow field. Inaccuracies in estimating the center of rotation result in a predictable systematic error when one is estimating local angular velocity. Our results show that humans make the predicted errors. We discuss how the brain might estimate the elementary components of the optic flow locally by using large receptive fields. © 2003 Optical Society of America

*OCIS codes:* 000.330, 330.4150, 330.4060.

## 1. INTRODUCTION

Optic flow generated on our eyes as objects move or as we move through the environment is a rich source of information for orientation, navigation, and the perception of the three-dimensional world.<sup>1,2</sup> Koenderink and van Doorn<sup>2</sup> showed that if these optic flows are generated by transformations of planar surfaces, then the flows can be decomposed in terms of a few elementary motions, including translation, expansion, and rotation. Because small patches of natural surfaces are approximately planar, it may be possible to perform this decomposition for small portions of natural images. Recent theoretical work showed how to perform this decomposition in a Bayesian manner.<sup>3</sup> This new theory proposes that the visual system fits internal models to the incoming retinal data, selecting the best models and their parameters. The fit begins with a measurement stage that performs local estimates of motion, such as local velocity. These local estimates are then clustered in a space of measurement variables. The clusters form regions, whose boundaries correspond to motion boundaries. Clustering is performed by a number of competitive processes corresponding to different motions. The theory proposes that different types of tests can perform this clustering. For example, the grouping can be done by either parametric or nonparametric tests. The former will try to detect familiar motions defined by prior statistics-of-natural-scenes models. In turn, the latter will allow the visual system to deal with general types of motion that may never have been seen before. Although knowledge of motion statistics in natural images is important for understanding what these familiar motions are, the theoretical studies of Koenderink and van Doorn can illuminate this issue.

Brains take advantage of such theoretical decomposi-

tion of the optic flow as they estimate things such as the velocity of translation<sup>4,5</sup> and the angular velocity of rotation.<sup>6</sup> Further evidence for such decomposition comes from some recent apparent-velocity experiments,<sup>7-9</sup> which could be explained only by using some form of global-velocity information.<sup>10</sup> Furthermore, the proposal of such specialized mechanisms is consistent with psychophysical studies suggesting the existence of looming and rotation detectors<sup>11-13</sup> working independently,<sup>14</sup> and several physiological studies in primates have shown that there are cortical neurons sensitive to translation, rotation, expansion, and spiral motion.<sup>15-21</sup> Cells sensitive to optic-flow components were also found in flies<sup>22</sup> and pigeons.<sup>23</sup> However, the decomposition of optic flow into elementary motion components is useful only if it is local. This is because the decomposition is unique only for planar patches in the world, that is, for small pieces of surfaces.<sup>2</sup> In this paper we focus on angular velocity and show that its measurement is local, thus supporting a role for rotation in the putative decomposition.

Our argument begins with a recent study in which we showed that humans can make independent estimates of angular velocity for different parts of an image.<sup>6</sup> In that study, a rotating random-dot disk was presented to the subjects. The disk was such that the directions of motion of the dots were consistent with rotation, but the speed of all dots was the same regardless of the distance from the center of rotation. The percept was of a coherent non-rigid rotation such that the inner portions of the disk seemed to rotate faster than its outer portions. We then measured the perceived angular velocity as a function of the distance from the center of rotation<sup>6</sup> we found that this velocity was equal to the local speed divided by the distance, implying that the brain does not compute a single global estimate of angular velocity but appears to

compute it point by point. If this is the case, then the perception of angular velocity should depend strongly on the estimate of the center of rotation. If the estimate of the center of rotation were incorrect, then so would be the angular velocity in a predictable manner.

To test the dependence of the angular velocity on the estimated position of the center of rotation, we took advantage of some preliminary results,<sup>24</sup> which we expanded upon and present here. These results show that humans make errors in the estimate of the center of rotation. Given these errors, where does the brain place the center of rotation for computing local angular velocity? The best guess is that it is located near the fixation point, as thus the bulk of the sensory data would fall on the fovea. We therefore predicted that if the center of rotation were away from the fixation point, then humans would make systematic errors in the estimation of angular velocity. More precisely, we predicted that angular velocities would be overestimated, because the speeds near the presumed center of rotation would not be near zero, as is the case for rotations. This is the prediction that we tested in our experiments.

## 2. METHODS

### A. Stimuli

Stimuli consisted of random-dot patterns undergoing rotation, displayed in a square patch, whose size was  $20 \times 20 \text{ deg}^2$ . An illustration of the stimuli appears in Fig. 1, with the white square representing the actual center of rotation and the plus sign indicating the fixation point. Line segments indicate the flow of the pattern, with their lengths being proportional to the speed of the dots. The dot density ( $0.275 \text{ dot deg}^{-2}$ ) was homogeneous across the field. The size of the dots was 11 arc min, and they were displayed with a luminance of  $19.5 \text{ cd}$

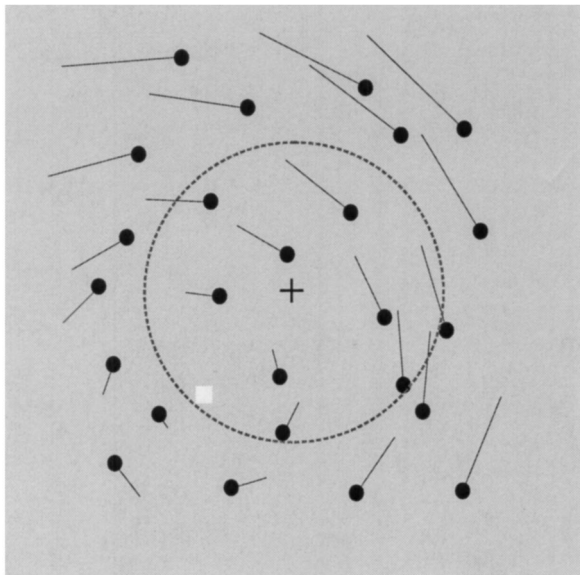


Fig. 1. Schematics of a random-dot pattern undergoing rotation, with the center of rotation (white square) deviated from the center of the stimulus, which coincides with the fixation point (plus sign). The large dashed circle indicates the part of the stimulus covered by the mask.

$\text{m}^{-2}$  on a background whose luminance was  $39 \text{ cd m}^{-2}$ . To avoid dot tracking and facilitate fixation, the dots were displayed for only three frames and then replotted at random positions. In the first frame of the stimulus presentation, each dot was randomly assigned a lifetime between one and three frames so that they would not be replotted all at the same time, thereby producing flicker. Stimuli were displayed on a high-resolution CRT monitor at a frame rate of 62 Hz.

### B. Procedure

Four different kinds of experiment were performed in this study. In the first kind, we explored the ability of the visual system to locate the center of rotation. In each trial, the center of rotation was randomly placed in the 45-deg diagonal of one of four quadrants (down-left, down-right, top-left, and top-right). The subject had to indicate in which of these four quadrants the center of rotation was located by pressing the keys 1, 3, 7, or 9 on the numeric keyboard. We varied the deviation of the center of rotation from the fixation point to determine the minimum distance needed for the subject to perform the task efficiently. Each stimulus comprised a circular mask (with the background luminance) placed concentric with the center of the display. The purpose of the mask was to investigate whether the visual system uses the local information around the center of rotation for its localization. As we varied the size of the mask, the number of dots in the rest of the display was either kept constant or maintained at constant density. The distance thresholds were obtained by fitting Weibull functions to the proportion of correct answers. We obtained these thresholds for a set of six distances presented in each of two blocks of trials. Each distance appeared a total of 20 times per block. The presentation time for each condition was 18 frames long, and the angular velocity was  $72 \text{ deg sec}^{-1}$ .

In the second kind of experiment, we measured the perceived angular velocity for different experimental conditions. The procedure for these experiments was as follows: Two stimuli (reference and test) were sequentially displayed during 193 ms (12 frames), a time sufficiently short to avoid a saccade during the presentation,<sup>25</sup> with an interstimulus interval of 516 ms (32 frames). The angular velocity of the reference stimulus was  $100 \text{ deg sec}^{-1}$ , while that of the test varied. In the reference stimulus, the center of rotation was located on the geometric center of the stimulus, which coincided with the fixation point. On the other hand, in the test stimulus, the center of rotation (condition A), the fixation point (condition C), or both (condition B) were deviated from the center of the stimulus. The subject had to indicate by pressing a mouse button which of the stimuli, first or second, rotated faster. The order of presentation of the reference and test stimuli was random. We used a two-alternative forced-choice paradigm with the method of constant stimuli to obtain the subjects' psychometric functions. The matching velocity was calculated by fitting cumulative Gaussian curves to these functions. To obtain these functions, a set of six stimuli was used in each of two blocks of trials. Each stimulus appeared a total of 20 times per block.

In the third kind of experiment, we investigated the effect of masking the stimulus on the perceived angular velocity for condition A. The masks were identical to those described for the first kind of experiment. In this case, the experiment was performed by keeping only the density constant.

In the fourth kind of experiment, we measured the perceived center of rotation when it was deviated from the fixation point. We presented to the subjects a random-dot pattern undergoing rotation whose center of rotation was randomly located along the horizontal line crossing the fixation point, on the right side of the display. The stimulus duration was identical to that used in the velocity-discrimination experiments. After the stimulus disappeared, a zero-to-five numbered ruler was displayed during 193 ms (12 frames) along the segment of the horizontal line where the center of rotation was located. The ruler had six marks (including the fixation mark) separated 2 deg from one another. Subjects were required to use the ruler for their position judgment of the center of rotation.

**C. Subjects**

Four experienced subjects participated in these experiments, one of the authors and three others naive as to the purpose of the study. Viewing was binocular, with natural pupils.

**3. RESULTS**

**A. Experiment 1: Estimate of the Center of Rotation**

We measured the minimum deviation of the center of rotation from the fixation point needed for the subject to locate the position of this center in one of four quadrants. To investigate whether the visual system uses the local information around the center of rotation to estimate its position, some of the experimental conditions masked a region around the center of rotation. To control for a possible effect of the number of dots in the masking condition, we performed the experiment by keeping constant either the number or the density of the dots in the visible part of the stimulus.

Figure 2 shows the deviation threshold as a function of the mask radius for both constant number of dots and constant density. The results show that for our experimental conditions, the center of rotation is misjudged by at least 1.3 deg. The estimation performance can be poorer than that. Estimation thresholds were much higher before training (solid circles) for both subjects. These high thresholds may be due to the visual system not using all the information about the rotation. The flatness of the curves in Fig. 2 supports this hypothesis by showing that the visual system may not use the information around the center itself to estimate its position, because otherwise, this estimate would depend strongly on the size of the mask.

**B. Experiment 2: Effect of Mislocating the Center of Rotation on the Perceived Angular Velocity**

We investigated how mislocating the center of rotation affects the perceived angular velocity. We did so by deviating the center of rotation from the center of the display

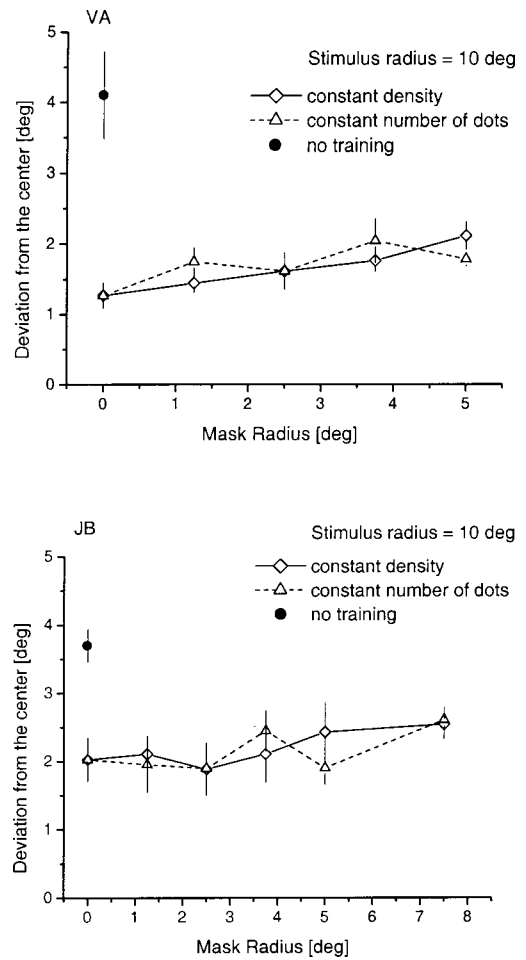


Fig. 2. Position estimation of the center of rotation as a function of the mask radius. The two graphs correspond to results from two subjects. Each graph shows the results for three conditions: with no training on the task and with training and either the density or the number of dots constant outside the mask. Even trained subjects could not estimate the center of rotation precisely with this task. Before training, errors were much higher for both subjects (solid circles). Finally, the errors do not increase significantly with the radius of the mask.

(condition A), where the fixation point was located (see Fig. 1). Figure 3 plots the ratio between matching and reference angular velocities as a function of the distance between the center of rotation and the fixation point. Results show that subjects overestimate angular velocity under this condition and that this overestimation increases with distance. This result is consistent with our prediction about how the perceived angular velocity depends on the estimate of the center of rotation.

However, this experiment does not rule out the possibility that the visual system uses a geometric clue such as the center of the display and not the fixation point as the perceived center of rotation. Another possibility is that the perceived center of rotation lies between the actual center of rotation and the fixation point. To evaluate these possibilities, we conducted the same experiment under two new conditions. In condition B, both the center of rotation and the fixation point were deviated from the geometric center of the display and located in the same position. In condition C, the fixation point but not the center of rotation was deviated from the geometric center

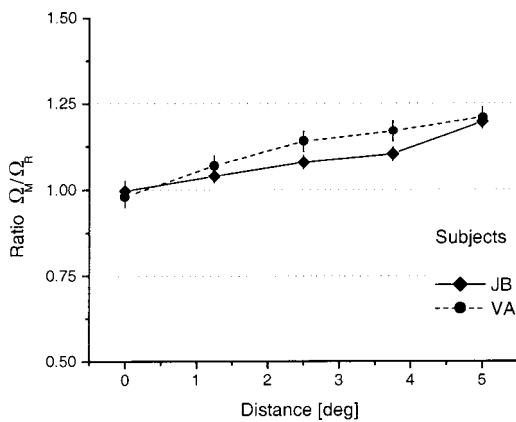


Fig. 3. Ratio between matching ( $\Omega_M$ ) and reference ( $\Omega_R$ ) angular velocities as a function of the distance from the center of rotation to the fixation point. The two curves correspond to results from two subjects. The plot shows that subjects overestimate angular velocity when the center of rotation is different from the fixation point and that this effect increases with distance.

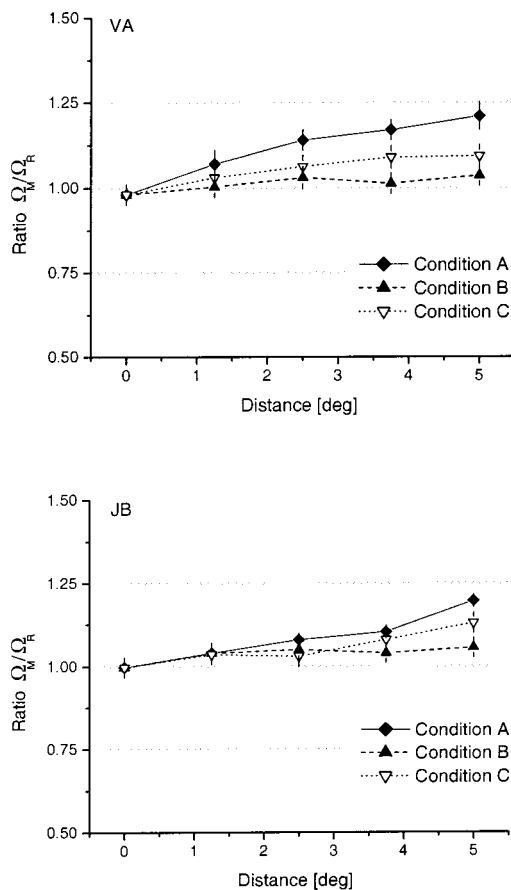


Fig. 4. Comparison of perceived angular velocity across three different conditions. Condition A (diamonds and solid curve) corresponds to the center of rotation being deviated from the center of the stimulus, where the fixation point is located. Condition B (solid triangles and dashed curve) corresponds to the center of rotation being deviated from the center of the stimulus and the fixation point being located on the center of rotation. Condition C (open triangles and dotted curve) corresponds to the center of rotation being located on the center of the stimulus and the fixation point being deviated from the center. The two panels show results from two subjects.

of the display. Figure 4 plots the ratio between matching and reference angular velocities as a function of distance. This distance is between the fixation point and the geometric center of the display for condition B and between the center of rotation and the fixation point for condition C. Results show that when the fixation point and the center of rotation do not coincide, subjects overestimate angular velocity (the solid curve represents results of condition A and the dotted curve results of condition C). In contrast, when the fixation is located on the actual center of rotation, subjects estimate the correct angular velocity, ruling out the possibility that the visual system uses the geometrical center of the display as the perceived center of rotation in this experiment (dashed curve). We hypothesize that when the center of rotation and the fixation point do not coincide, the perceived location of the former is biased toward the latter, causing the error in the estimate of angular velocity. It is interesting that the overestimation measured in condition A was greater than that found in condition C. This could be due to the differences in the distributions of velocities in both stimuli. When the center of rotation is shifted to one side of the geometric center, higher angular velocities appear on the other side of it than appear when the rotation is centered, as in condition C.

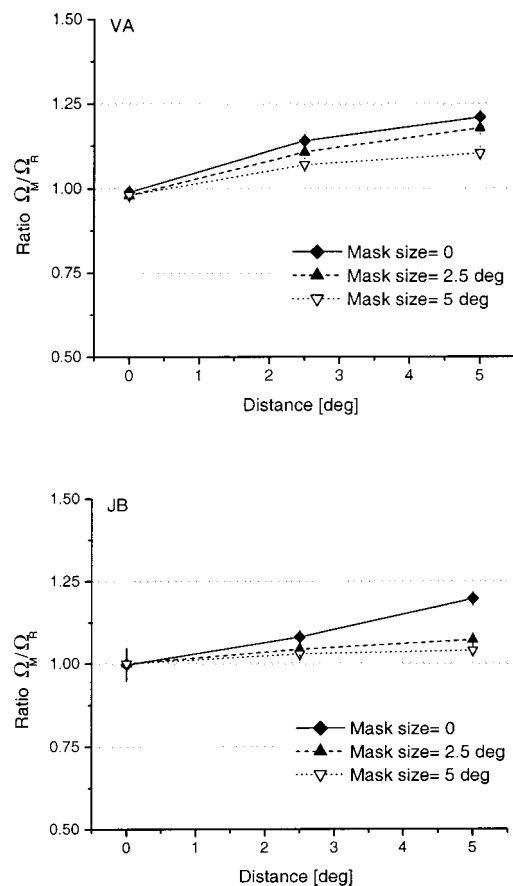


Fig. 5. Effect on the overestimation of angular velocity of masking the portion of the stimulus around the fixation point. The two panels show results from two subjects. Masking reduces the overestimation, and this effect increases with the size of the mask.

**C. Experiment 3: Effect of Masking on the Perceived Angular Velocity**

If the angular velocity were computed locally, then a dislocation of the center of rotation would result in high estimates of angular velocity for those points near the perceived center of rotation. In other words, the largest errors in the estimate of angular velocity would be committed near the fixation point. If this prediction is correct, then removing dots near the fixation point from the stimulus should produce a decrease in the overestimation of angular velocity. We tested this prediction by masking a region around the fixation point with a disk with the background luminance. We then measured the perceived angular velocity for condition A and two values of mask radius. Results (Fig. 5) show that the overestimation of angular velocity decreases dramatically when the central part of the stimulus is masked, suggesting that the overestimation is caused mainly by the angular velocity estimates around the perceived center of rotation.

**4. MODEL**

The analysis of rotational motion begins with local measurements of velocity. These measurements are then integrated to generate a more global description of the motion. If one thinks that these local measurements are noisy and sometimes ambiguous,<sup>26</sup> the best way to use them would be to construct a rotational vector field that best fits them and find the angular velocity corresponding to this fit. However, such a fitting model would fail to describe nonrigid rotations.<sup>6</sup> An alternative model favored by our data is to compute the angular velocities in small patches of the image and then integrate them in such a way as to generate a more complex description of the rotational field. This model would allow us not only to compute a global value of angular velocity but also to explain these percepts produced by local differences in angular velocity such as in nonrigid rotations.

The model presented here follows a Bayesian framework developed recently.<sup>3</sup> One can cast models in that framework through either maximization of probabilities or minimization of energy functions. Here we follow the energy-minimization approach, as it lends itself to more-intuitive explanations of the computation. Our model performs this computation in two stages. In the first stage, the model assumes a center of rotation and computes a value of angular velocity at each point of the image on the basis of measurements of local linear velocity. These local measurements are assumed to be veridical for the purpose of the model. This assumption is valid, as the human visual system can discriminate velocities that are just 5% different.<sup>4</sup> The discrimination uses mechanisms tuned to speed and direction of motion that allow the representation of local image velocities.<sup>27</sup> There are several physiological models for these mechanisms<sup>28-31</sup> based on the distributed outputs of motion-energy units tuned to different spatial and temporal frequencies. These models can successfully explain how the brain performs local-velocity measurements.

The local computations of angular velocity are done by using the projections of the local-velocity vectors onto the theoretical direction of the vectors corresponding to the

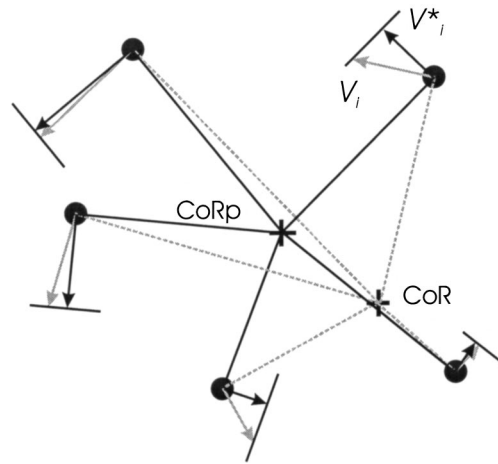


Fig. 6. Schematic of how the first stage of the model works. The actual and the perceived center of rotation (CoR and CoRp, respectively) are in different positions. Consequently, the generated local velocities ( $v_i$ , solid gray vectors) at positions  $r_i$  are not compatible with a rotation about the perceived center of rotation. The model seeks local vectors ( $v_i^*$ , solid black vectors) that are as consistent as possible with the measured velocities and with a rotation about the perceived center. These vectors tend to be projections of  $v_i$  onto lines perpendicular to  $r_i$ .

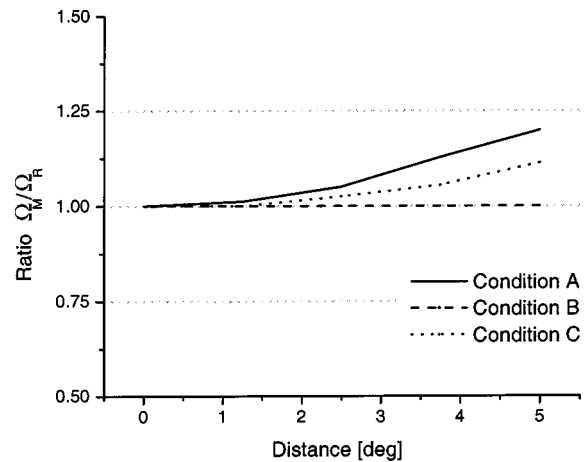


Fig. 7. The model accounts for the experiment in which the effect of mislocating the center of rotation on perceived angular velocity is studied (see Fig. 2).

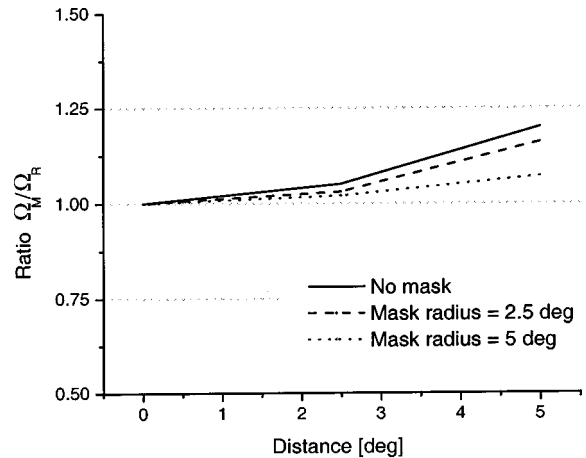


Fig. 8. The model accounts for the experiment in which the effect of masking the portion of the stimulus around the fixation point is studied (see Fig. 3).

rotation (Fig. 6). This is equivalent to minimizing the discrepancies between vectors expected by the rotation and measured local-velocity vectors [see Eq. (A1) in Appendix A]. In the second stage, the local measurements of angular velocity are combined by computing their median. This median is weighed in such a way as to emphasize the local measurements coming from the fovea. We use this weighed median, because we assume that measurements from the periphery are less reliable. One can model this median computation with a smoothing mechanism [Eq. (A2)]. This mechanism has a parameter  $\lambda$  that can be interpreted as the relative weight of smoothing compared with the reliability of the local angular-

velocity measurements. Large values of  $\lambda$  mean that the system does not rely on the local measurements of angular velocity because of their poor quality. In this case, the smoothing term would impose a constant value of angular velocity across the image. On the other hand, when  $\lambda$  is small, the model can capture nonrigid portions of the image.

**A. Simulations**

Figure 7 shows the results of the simulations with the local angular-velocity model in which the effect of the mislocation of the center of rotation on the perceived angular

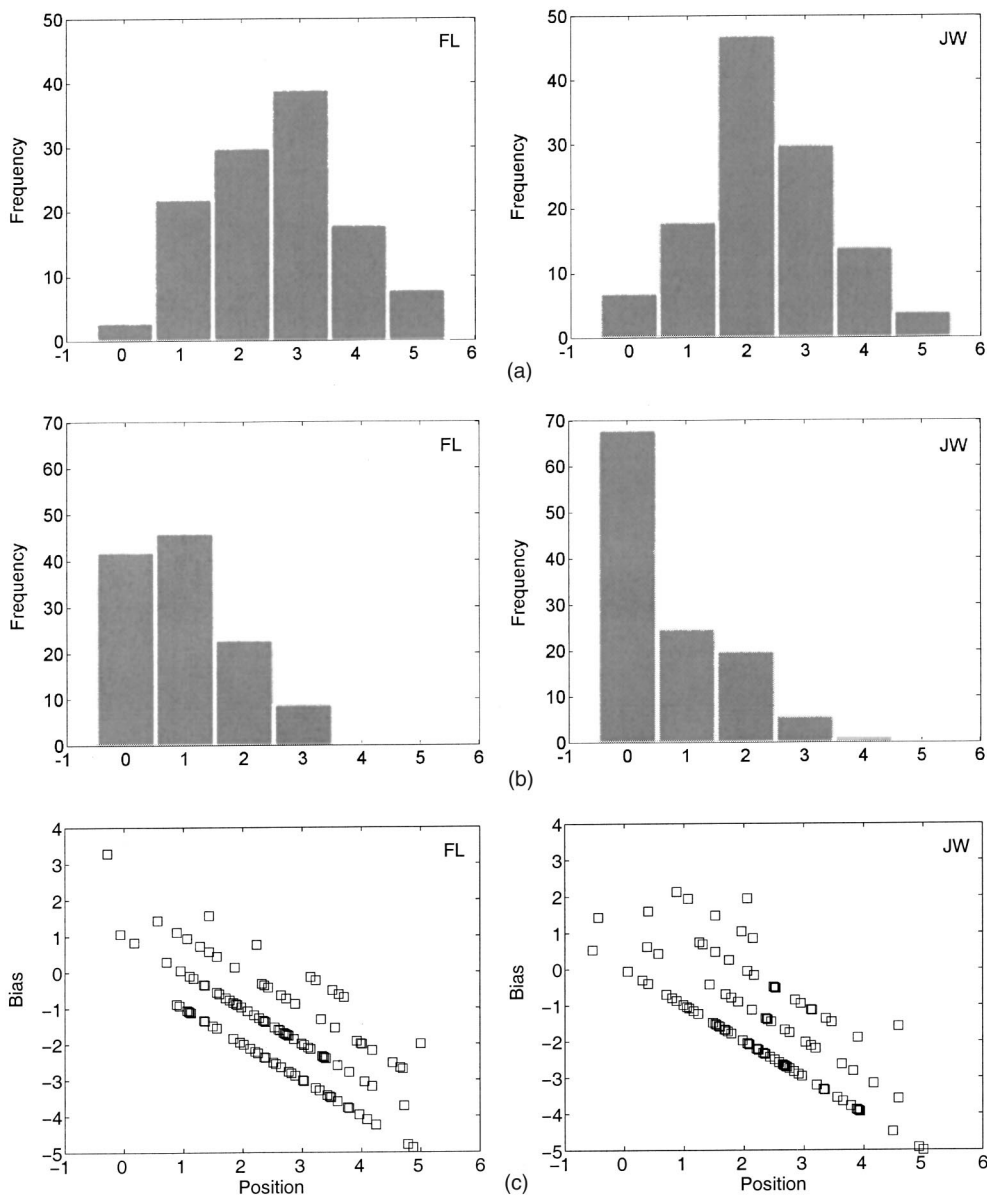


Fig. 9. Estimates of perceived center of rotation. (a) Distribution, for two subjects, of actual positions of the center of rotation with respect to the fixation point. The position scale corresponds to the ruler used in the experiment. In degrees, the position could take any value between 0 (the fixation point) and 10 (the border of the display). (b) Estimated position of the center of rotation, for two subjects. There is a shift of the distribution of estimated positions toward zero (fixation point) in comparison with the distribution of actual positions. (c) Bias as a function of the actual position of the center of rotation, computed as the difference between the estimated and the actual positions. The plots show, for both subjects, that in most trials the subject saw the center of rotation biased toward the fixation point. Moreover, the bias has a negative linear correlation with the distance from the fixation point.

velocity is studied (see Fig. 3 and 4). Results show that the model accounts for the overestimation of angular velocity for both situations in which the center of rotation and the fixation point do not coincide and a correct estimate when these points coincide. The simulations also show that the maximum of overestimation reaches approximately 20% for condition A and 10% for condition B, which is consistent with the experimental data. Figure 8 shows the simulations of the masking experiment (see Fig. 5). The model accounts for the reduction of the overestimation of angular velocity with masking and for the magnified reduction as the mask increases.

The model as implemented here has two free parameters. The first is the position of the perceived center of rotation between fixation and the actual center of rotation. The second is the standard deviation  $\sigma$  of the weighting function in Eq. (A2). This weighting function expresses the portion of the visual field emphasized by the computation, that is, the portion sufficiently close to the fovea. The best result was obtained by placing the perceived center of rotation at one third of the way between the fixation point and the actual center of rotation and by setting  $\sigma$  of the weighting function at 5.5 deg. Both parameters were robust, admitting a variation of the order of 20%.

## B. A Test of the Model

The success of the simulations suggests that the estimated center of rotation is between the actual center and the fixation point. We tested this prediction with an experiment in which two naïve subjects were asked to make subjective estimates of the center of rotation in a display similar to that used in the previous experiments. Figure 9(a) shows the actual random distributions of locations of the center of rotation, and Fig. 9(b) shows how the subjects estimated the position of the center of rotation. The estimates are significantly shifted to the left, having their maximum near zero. Hence, consistently with the prediction of the model, subjects perceive the center of rotation biased toward the fixation point. Figure 9(c) shows the bias computed as the difference between the estimated and the actual positions of the center as a function of the actual position. Biases toward the fixation are represented in this figure by negative values. Most data points are negative, confirming these biases. Moreover, they show a negative linear correlation with position. This correlation suggests that the bias depends on the relative distance from the fixation point. This dependence is an interesting result that is also predicted by the model. In it, the distance of the estimated center of rotation to the fixation point is always a fraction of the distance of the actual center of rotation to the fixation point.

## 5. DISCUSSION

In this paper we have discussed two pieces of evidence that angular velocity is computed locally. The first came from measurements of angular velocity at different positions of a nonrigid rotation (Ref. 6, Fig. 5). The second came from the errors that observers make when the center of rotation does not coincide with the fixation point. What are the advantages of a local computation of angu-

lar velocity? One advantage would be a relatively small computational cost compared with that from a mechanism that fits the best overall angular velocity to the local-velocity data. (One can estimate this cost in terms of the number of multiplications needed to compute angular velocity. Because our model uses local computations and the median, it needs fewer multiplications than a model that fits a rotational vector field globally to the data.) But the main advantage is allowing the brain to decompose<sup>3</sup> complex optic flow into the elementary motion components outlined by Koenderink and van Doorn.<sup>2</sup> As explained in Section 1, such decompositions would be possible for small portions of natural optic flow and might thus be amenable to a Bayesian treatment. Our model follows a recently proposed framework for such a treatment.<sup>3</sup> However, a surprise in terms of this framework is that the visual system does not estimate the center of rotation well. In principle, models based on the framework could perform such estimations. That the brain does not perform them suggests an implementational difficulty, such as an inability to measure the slow velocities near the center of rotation.<sup>4</sup> Such a difficulty can be incorporated into the framework through an appropriate likelihood function. Finally, although our model applies only to rotations, one can extend it with the framework to encompass complex optic flow. This is important because pure two-dimensional rotations are rare in natural images and occur mostly in combination with other motions.

Here we propose a model for the computation of rotational motions that is based on two stages: a stage estimating local angular velocities and an integration stage. A related finding is that the perception of angular velocity is constrained by the estimate of the center of rotation. In the first stage of the model, this estimate is used to compute local angular velocities from the local measurements of linear velocity. The estimate of the center of rotation could be instantiated by using mechanisms similar to those proposed for heading direction.<sup>32,33</sup> In turn, local measurements of linear velocity could be performed by population coding, as in certain models of the physiology of motion mechanisms.<sup>28-31,34</sup> Finally, cells in area MST that are sensitive to complex motions<sup>16-19</sup> are good candidates for extracting local angular velocities or implementing the integration stage. They may be good integrators by virtue of the large size of their receptive fields. Their mean diameter is  $\sim 40$  deg, independently of eccentricity.<sup>35</sup> In turn, some of these cells could compute angular velocity, as they are selective to two-dimensional rotations or spirals.<sup>16-21</sup> However, although they respond to the direction of rotation, it is still unclear whether different rotation or spiral selective cells are selective for different angular velocities. Moreover, one must solve the problem of how these cells compute angular velocity locally. One possibility is that they tile space with some overlap, with location being indicated by relative firing across the population of cells. A problem with this tiling hypothesis is that large receptive fields may cover different portions of the image that have different angular velocities, confounding them. Fortunately, the variance in receptive-field sizes is large,<sup>36</sup> allowing tilings of different spatial resolutions, including some fine ones.

One important issue that was raised by our model is the choice of the balance between respecting local measurements and imposing integration. In this study we tipped the balance toward integration, because there was uncertainty about the estimation of the center of rotation. Therefore the system should not rely much on the local measurements of angular velocity, and the integration (smoothing) should dominate. This presumed smoothing was consistent with the rigid rotations that subjects perceived in all our experimental conditions. However, a remaining fascinating question is how the brain balances rigidity and nonrigidity when facing natural optic flow.

## APPENDIX A

Our model follows the energy-minimization formulation of a recent Bayesian framework for the perception of visual motion.<sup>3</sup> In its first stage, this model computes a local value of angular velocity for each point of the image. Figure 6 shows schematically the proposed computation, which is formalized as

$$\Omega_l(\mathbf{r}_i) = \arg \min_{\Omega^*, \nu_i^*} \left[ \sum_{i=1}^N |\nu_i - \nu_i^*| + k \sum_{i=1}^N |\Omega^*(\mathbf{r}_i) \times \mathbf{r}_i - \nu_i| \right], \quad (\text{A1})$$

where  $\Omega_l$  is the computed local angular velocity at position  $\mathbf{r}_i$ ,  $\nu_i$  is measured linear velocity at the same position, and  $N$  is the number of dots in the display. The first term on the right-hand side of this equation tries to enforce the local measurements of linear velocity, while the second term imposes a rotational motion. The positive parameter  $k$  quantifies the relative trust in these kinds of motion. It is in the  $k$  term of the equation that we enforce the minimization over  $\Omega^*$ . This variable is the angular velocity vector at position  $\mathbf{r}_i$ . The result of the cross product  $\Omega^*(\mathbf{r}_i) \times \mathbf{r}_i$  is a velocity vector that lies on the same plane as  $\nu_i$ . The model minimizes the difference between these two velocity vectors. As is shown in Fig. 6, the minimum is reached when  $\Omega^*(\mathbf{r}_i) \times \mathbf{r}_i$  equals the projection of  $\nu_i$  onto a line perpendicular to  $\mathbf{r}_i$ .

Once the local angular velocities of rotation are computed, the model combines them as follows:

$$\Omega(\mathbf{r}_i) = \arg \min_{\Omega^*} \left\{ \sum_{i=1}^N \exp\left(-\frac{\epsilon_i^2}{2\sigma^2}\right) |\Omega^*(\mathbf{r}_i) - \Omega(\mathbf{r}_i)| + \lambda \int_{\mathbf{r}} [D(\Omega^*(\mathbf{r}))]^2 \right\}. \quad (\text{A2})$$

The first term on the right-hand side of this equation is equivalent to trying to enforce the computation of a weighed median across the image.<sup>36</sup> The exponential is the function that assigns a weight to each  $i$ th position in the image depending on its eccentricity  $\epsilon$ . This is a Gaussian function with the mean located on the fixation point and standard deviation  $\sigma$ . Such a weighing function enforces that foveal data are more reliable than peripheral data. The second term smoothes the motion across locations in the image. The operator  $D$  is a differ-

ential operator that should contain derivatives of many orders<sup>37</sup> and, in particular, should contain first-order derivatives so that the  $\Omega^*$  that minimizes the integral can be constant across  $\mathbf{r}_i$  (rigidity condition). [One can modify Eq. (A2) to take into account optic-flow discontinuities,<sup>3</sup> but this is outside the scope of this paper.]

For the simulations here, we set  $k$  and  $\lambda$  to very large values, as the percepts were of rigid rotational motion. Therefore, Eqs. (A1) and (A2) could be reduced to

$$\Omega_l(\mathbf{r}_i) = \arg \min_{\Omega^*} \left[ \sum_{i=1}^N |\Omega^*(\mathbf{r}_i) \times \mathbf{r}_i - \nu_i| \right], \quad (\text{A1b})$$

and

$$\Omega = \arg \min_{\Omega^*} \left[ \sum_{i=1}^N \exp\left(-\frac{\epsilon_i^2}{2\sigma^2}\right) |\Omega^* - \Omega_l(\mathbf{r}_i)| \right], \quad (\text{A2b})$$

respectively, and the model computes a single value of angular velocity for the whole image.

## ACKNOWLEDGMENTS

We thank the reviewers for their useful comments, in particular for the suggestion of the experimental control for the model, which notably enhanced this paper. This work was supported by National Eye Institute grants EY08921 and EY11170.

Correspondence should be addressed to N. M. Grzywacz at nmg@bmsr.usc.edu.

## REFERENCES

1. J. J. Gibson, *The Perception of the Visual World* (Houghton Mifflin, Boston, Mass., 1950).
2. J. J. Koenderink and A. J. van Doorn, "Local structure of movement parallax of the plane," *J. Opt. Soc. Am.* **66**, 717–723 (1976).
3. A. L. Yuille and N. M. Grzywacz, "A theoretical framework for visual motion," in *High-Level Motion Processing—Computational, Neurobiological, and Psychophysical Perspectives*, T. Watanabe, ed. (MIT Press, Cambridge, Mass., 1998), pp. 187–211.
4. S. P. McKee, "A local mechanism for differential velocity detection," *Vision Res.* **21**, 491–500 (1981).
5. A. Johnston, C. P. Benton, and N. J. Morgan, "Concurrent measurement of perceived speed and speed discrimination using the method of single stimuli," *Vision Res.* **39**, 3849–3854 (1999).
6. J. F. Barraza and N. M. Grzywacz, "Measurement of angular velocity in the perception of rotation," *Vision Res.* **42**, 2457–2462 (2002).
7. P. J. Bex and W. Makous, "Radial motion looks faster," *Vision Res.* **37**, 3399–3405 (1997).
8. B. J. Geesaman and N. Qian, "A novel speed illusion involving expansion and rotation patterns," *Vision Res.* **36**, 3281–3292 (1996).
9. B. J. Geesaman and N. Qian, "The effect of complex motion pattern on speed perception," *Vision Res.* **38**, 1223–1231 (1998).
10. C. W. G. Clifford, S. A. Beardsley, and L. M. Vaina, "The perception and discrimination of speed in complex motion," *Vision Res.* **39**, 2213–2227 (1999).
11. D. Regan and K. J. Beberley, "Visual responses to vorticity and the neural analysis of optic flow," *J. Opt. Soc. Am. A* **2**, 280–283 (1985).
12. T. A. C. Freeman and M. G. Harris, "Human sensitivity to

- expanding and rotating motion: effects of complementary masking and directional structure," *Vision Res.* **32**, 81–87 (1992).
13. M. C. Morrone, D. C. Burr, and L. M. Vaina, "Two stages of visual processing for radial and circular motion," *Nature* **376**, 507–509 (1995).
  14. S. F. de Pas, A. M. L. Kappers, and J. J. Koenderink, "Detection of first-order structure in optic flow fields," *Vision Res.* **36**, 259–270 (1996).
  15. J. H. R. Maunsell and D. C. Van Essen, "Functional properties of neurons in middle temporal visual area of the macaque monkey. I: selectivity for stimulus direction, speed, and orientation," *J. Neurophys.* **49**, 1127–1147 (1983).
  16. A. Tanaka and H. Saito, "Analysis of motion of the visual field by direction, expansion/contraction, and rotation cells clustered in the dorsal part of the medial superior temporal area of the macaque monkey," *J. Neurophys.* **62**, 626–641 (1989).
  17. A. Tanaka, Y. Fukuda, and H. Saito, "Underlying mechanisms of the response specificity of expansion/contraction, and rotation cells, in the dorsal part of the medial superior temporal area of the macaque monkey," *J. Neurophys.* **62**, 642–656 (1989).
  18. C. J. Duffy and R. H. Wurtz, "Sensitivity of MST neurons to optic flow stimuli. I. A continuum of response selectivity to large-field stimuli," *J. Neurophys.* **65**, 1346–1359 (1991).
  19. C. J. Duffy and R. H. Wurtz, "Sensitivity of MST neurons to optic flow stimuli. II. Mechanisms of response selectivity revealed by small-field stimuli," *J. Neurophys.* **65**, 1346–1359 (1991).
  20. M. S. A. Graziano, R. A. Andersen, and R. J. Snowden, "Tuning of MST neurons to spiral motions," *J. Neurosci.* **14**, 54–67 (1994).
  21. G. A. Orban, L. Lagae, A. Verri, S. Raiguel, D. Xiao, H. Maes, and V. Torre, "First-order analysis of optical flow in monkey brain," *Proc. Natl. Acad. Sci. USA* **89**, 2595–2599 (1992).
  22. M. Egelhaaf, R. Kern, H. G. Krapp, J. Kretzberg, and A. Warzecha, "Natural encoding of behaviourally relevant visual-motion information in the fly," *Trends Neurosci.* **25**, 96–102 (2002).
  23. D. R. W. Wylie, W. F. Bischof, and B. J. Frost, "Common reference frame for neural coding of translational and rotational optic flow," *Nature* **392**, 278–282 (1998).
  24. J. F. Barraza and N. M. Grzywacz, "Fine discrimination of angular velocity despite poor localization of center of rotation," presented at Vision Sciences Society 2nd Annual Meeting, Sarasota, Florida, May 10–15, 2002.
  25. M. E. Goldberg, H. M. Eggers, and P. Gouras, "The ocular motor system," in *Principles of Neural Science*, E. R. Kandel, J. H. Schwartz, and T. M. Jessell, eds. (Appleton & Lange, Norwalk, Conn., 1991), pp. 660–677.
  26. A. Movshon, E. Adelson, M. Gizzi, and W. Newsome, "The analysis of moving visual patterns," *Exp. Brain Res.* **11**, 117–152 (1986).
  27. P. R. Schrater and E. P. Simoncelli, "Local velocity representation: evidence from motion adaptation," *Vision Res.* **38**, 3899–3912 (1998).
  28. D. Ascher and N. M. Grzywacz, "A Bayesian model for the measurement of visual velocity," *Vision Res.* **40**, 3427–3434 (2000).
  29. S. J. Nowlan and T. J. Sejnowski, "A selection model for motion processing in area MT of primates," *J. Neurosci.* **15**, 1195–1214 (1995).
  30. E. Simoncelli and D. Heeger, "A model of neural responses in visual area MT," *Vision Res.* **38**, 743–761 (1998).
  31. N. M. Grzywacz and A. L. Yuille, "A model for the estimate of local image velocity by cells in the visual cortex," *Proc. R. Soc. London Ser. B* **239**, 129–161 (1990).
  32. J. A. Perrone, "Model for the computation of self-motion in biological systems," *J. Opt. Soc. Am.* **A9**, 177–194 (1992).
  33. B. P. Dyre and G. J. Andersen, "Image velocity and perception of heading," *J. Exp. Psychol. Hum. Percept. Perform.* **23**, 546–565 (1997).
  34. J. A. Perrone and A. Thiele, "Speed skills: measuring the visual speed analyzing properties of primate MT neurons," *Nat. Neurosci.* **4**, 526–532 (2001).
  35. S. Raiguel, M. M. Van Hulle, D. K. Xiao, V. L. Marcar, L. Lagae, G. A. Orban, "Size and shape of receptive fields in the medial superior temporal area (MST) of the macaque," *NeuroReport* **8**, 2803–2800 (1997).
  36. D. C. Hoagling, F. Mosteller, and J. W. Tukey, "Introduction to more refined estimators," in *Understanding Robust and Exploratory Data Analysis*, D. C. Hoagling, F. Mosteller, and J. W. Tukey, eds. (Wiley, New York, 1983), pp. 283–296.
  37. A. L. Yuille and N. M. Grzywacz, "A mathematical analysis of the motion coherence theory," *Int. J. Comput. Vision* **3**, 155–175 (1989).